Laser-Raman and atomic force microscopy assessment of the chlorococcalean affinity of problematic microfossils

Barbara Kremer[1*], Michael Bauer[2,3], Robert W. Stark[3,4,5], Norbert Gast[2], Wladyslaw Altermann[6], Hans-Jürgen Gursky[7], Wolfgang M. Heckl[3,8,9] & Józef Kazmierczak[1]

[1] Institute of Paleobiology PAS, Twarda 51/55, 00-818 Warszawa, Poland
[2] Department of Earth and Environmental Sciences, LMU München, Theresienstr. 41, 80333 Munich, Germany
[3]Center for NanoScience (CeNS), Schellingstr. 4, 80799 Munich, Germany
[4] Institute of Materials Science, TU Darmstadt, Petersenstr. 32, 64287 Darmstadt, Germany
[5] Center of Smart Interfaces, TU Darmstadt, Petersenstr. 32, 64287 Darmstadt, Germany
[6] Department of Geology, University of Pretoria, South Africa
[7] Institute for Geology und Palaeontology, TU Clausthal, Leibnizstraße 10, 38678 Clausthal-Zellerfeld, Germany
[8] Deutsches Museum, Museumsinsel 1, 80538 Munich, Germany
[9] TUM School of Education, Technische Universität München, 80799 Munich, Germany

* corresponding author: kremer@twarda.pan.pl

Corresponding author:
tel. (+4822) 6978 886
fax. (+4822) 620 62 25
email: kremer@twarda.pan.pl

Organic-walled microfossils of uncertain origin, classified to an informal group named acritarchs, are most commonly interpreted as the resting cysts of marine eukaryotic phytoplankton. Some acritarchs have recently been interpreted as vegetative cells of chlorococcalean green algae, based on internal bodies that have been interpreted as their asexual reproductive structures (spores). To verify this interpretation, we applied confocal Raman spectroscopy and atomic force microscopy (AFM) to study the ultrastructure and nanostructure of exceptionally preserved acritarchs with internal bodies from the early Silurian cherts (c. 430 Ma-old) of Frankenwald (Germany). Three-dimensional Raman mapping showed the spatial distribution of carbonaceous material and other minerals in the walls of the analysed internal bodies and confirmed that these structures are comparable with spores of chlorococcalean microalgae. Our findings document therefore the oldest thus far known vegetative cells of sporulating green algae. The combination of confocal Raman and AFM techniques yielded detailed information about the nanostructure and fossilisation mode of the mineralised organic walls of both the central vesicles and the enclosed spore-like bodies.

Keywords: acritarch microfossils, mineralization, Silurian, Raman, AFM

Introduction

The informal taxonomic category of organic-walled microfossils named acritarchs[1] has an unclear systematic affiliation. They are traditionally interpreted as the cysts of unicellular organisms.[1,2] During the Proterozoic and Paleozoic, acritarchs formed the basis of the marine food chain and played an important role in the evolution of the global ecosystem. Acritarchs were therefore the main primary producers in the ocean for a long time and, as oxygenic microorganisms, they must have not only controlled the evolution of the marine ecosystem but also influenced planetary biochemical cycles. Acritarch-like fossils are among the oldest morphological traces of life[3], and the elucidation of their biological relationships sheds new light on the evolution of the early biosphere. It has recently been suggested that at least some acritarchs are the sporulating vegetative stages of unicellular green microalgae because they show internal bodies that can be interpreted as spores.[4]

The classification of acritarchs as green algae therefore has an important bearing on the overall understanding of basic processes in the evolution of Earth's biosphere. A precise morphological and chemical characterisation of acritarch internal bodies and of their three-dimensional arrangement is difficult because they are typically studied either in thin sections or after extraction from fossil-bearing rock. A detailed chemical or morphological study of microfossils usually requires physical or chemical preparation to extract the microfossils from the rock matrix, which can cause their partial or even total destruction. However, even the maceration process does not allow for extraction and study of these microfossils and their fragile internal bodies in a three-dimensional context.

During the last few years, acritarchs have been extensively examined in order to clarify their taxonomic position. In most common interpretations, they are considered metabolically inert resting stages of various algae.[5] Recent studies have shown that the acritarch wall ultrastructure can be single layered or multilayered.[6,7,8] Arouri et al.[9,10] studied the ultrastructure and chemistry of Neoproterozoic acritarchs from Australia and suggested a dinoflagellate affinity for the acanthomorph (process-bearing) forms with a multilayered, fibrillar wall, and a chlorophycean relationship to other taxa whose walls preserve a laminated organisation that is similar to the trilamellar structure (TLS) found in some extant green microalgae.[11,12] Recently, Kazmierczak and Kremer[4] described the internal bodies of a variety of early Silurian and late Devonian acritarchs and suggested that they were spores (autospores or aplanospores). The presence of spore-like bodies in acritarchs supports earlier explanations that some of them can be affined with unicellular green algae.[13,14,9,6,8] Although many sophisticated modern techniques have been applied in these studies[15,16,17], they have not unequivocally solved the question of biological affinity of acritarchs.

Thin sections of fossil-bearing rock can only provide a limited amount of detailed anatomical information. Although a thin planar section can be easily investigated optically, it provides minimal information about internal structures because only the projection of the object can be analysed. SEM techniques are limited to surface analysis and often require a conductive surface coating. Confocal microscopy is a potential solution to this dilemma because optical information can be gathered from below the surface of transparent specimens. Confocal Raman microscopy provides chemical and mineralogical information in addition to three-dimensional imaging. The confocal configuration utilises a small sample volume to record Raman scattering. Thus, lateral and vertical cross-sections can easily be generated with high spatial resolution. Raman spectroscopy has already shown its potential in palaeontology [18,19,16,20,21]: it is a non-destructive and non-intrusive spectroscopic technique that can be used to characterise the degree of geochemical maturity of organically-preserved microfossils along with the details of the embedding mineral matrix. Such analyses are important for, as an

example, verifying the biological or abiological origin of putative Archean microfossil-like structures.[19,22,23,24,25]. Two-dimensional images of microfossil-like objects and their embedding minerals can also provide evidence for the syngenicity of the studied objects with the surrounding rock.[20]

Raman mapping can be supplemented by high-resolution imaging with atomic force microscopy (AFM). In AFM, the sample surface is probed with a very sharp tip to provide a true three-dimensional surface profile. Imaging by AFM is non-destructive because it does not require any special surface treatment, such as coating or etching. The combination of AFM and Raman spectroscopy provides surface morphological information with nanometer resolution as well as the chemical information obtained by Raman spectroscopy.[18,26,27,28]

In the following, we discuss the nature and mode of preservation of the internal spore-like bodies of Silurian acritarch microfossils from southern Frankenwald, Germany (Fig. 1). The presence of such spore-like structures in the studied acritarchs is of critical importance for explaining their biological affinities. Green microalgae (Chlorococcales) are the only group of unicellular microalgae producing spores during asexual reproduction.[29] The only other group of extant unicellular algae reproducing also asexually by sporulation, are yellow-green algae (Xanthophyta). Their cell walls are, however, built of two overlapping halves, composed of easily degradable pectin, never supported by sporopollenin, and often containing silica[30]. Optical sections obtained with a confocal Raman microscope provide high-resolution data on the three-dimensional organisation of the internal bodies in situ. AFM data from the specimen surface complement this information. Raman data analysis revealed mineralisation of the organics with silica and iron oxide phases. In our opinion, the internal structures of the fossils are of paramount importance for understanding the biological affinities of at least some typical (spherical and acanthomorph)[31] representatives of these common Paleozoic and late Precambrian microorganisms, which undoubtedly represent the primary marine producers of their time period. To clarify the nature and fossilisation mode of these microfossils of unclear affiliation but high biostratigraphic relevance, we used *in situ*, non-destructive, high-resolution microscopy methods.

Material and Methods

Geological Setting

The acritarch-bearing rocks reported herein are representative of typical Paleozoic dark grey to black radiolarian cherts. In the European Silurian, such chert deposits occur in uplifted Variscan blocks[32], especially along the northwest rims of the Bohemian Massif (Germany) and the Holy Cross Mountains (Poland).

We refer to samples from the southern Frankenwald (Franconian Forest, northeast Bavaria, Germany, Fig. 1), where Silurian black cherts are distributed among several hundred minor occurrences and only a small number of easily accessible outcrops. Samples were derived from the abandoned gravel pit at Döbraberg (50°17’08,07” N; 11°39’24,02” E) in the area of village of Döbra near Schwarzenbach am Wald (Fig. 1), where a few metres of strongly deformed thin-bedded chert outcrop. For geographic and stratigraphic details see.[33,34,35] The cherts form faulted tectonic lenses, up to hundreds of metres long and tens of metres thick, and are set in a deformed regional “matrix” of Lower Carboniferous slates and greywackes with other lenses of variable Paleozoic rock units.

Methods

The early Silurian black cherts of Frankenwald, Germany contain rich and relatively well-preserved acritarchs. Petrographic thin sections with thicknesses of about 30 µm were prepared from these cherts. Specimens that contained well-preserved internal structures were selected with optical transmitted and reflected microscopy. Many specimens with a size of 30 to 50 µm contained multiple internal bodies with diameters ranging from 5 to 10 µm. The specimens were studied with optical microscopy (Zeiss Opton), scanning electron microscopy (SEM), confocal Raman spectroscopy and AFM. Petrographic thin sections of 30 µm thickness were polished, and some were slightly etched with 5% hydrofluoric acid. For SEM examination, the polished chert platelets were etched with 5% and 40% hydrofluoric acid and then sputtered with gold. The SEM examination was done with a Zeiss DSM 960A equipped with an EDS detector (Bruker axs) and a field-emission scanning electron microscope (JSM-7500F; Jeol, Japan).

The Raman spectra were acquired with a confocal Raman microscope (alpha300 R; WITec GmbH, Ulm, Germany). A frequency-doubled Nd:YAG laser (532 nm, P_{max} = 22.5 mW) was used for excitation. A 100× objective (Nikon, NA=0.90, 0.26 mm working distance) was used for excitation and collection of the scattered light in a backscattering geometry. The light was guided with a multimode optical fibre to the spectrometer using a 50-µm-diameter core as a pinhole for the confocal setup. The diffraction-limited focus resulted in a lateral resolution of about 400 nm with the confocal setup having a focal depth of 1 µm. Elastically scattered photons (Rayleigh scattering) and reflexion were rejected by a sharp edge filter. Entire spectra were acquired at each image point with a lens-based spectrometer with a spectral resolution of 3.51 cm^{-1} for the 600 mm^{-1} grating. Lateral and vertical distribution images were generated by sum filtering the counts in a selected range around a Raman peak for each spectrum.

Lateral and vertical 1 µm-thick optical slices were acquired with the Raman microscope from the surface to a maximum depth of 18 µm. The signal-to-noise ratio decreased significantly at about 5 µm and was not sufficient to allow for reliable three-dimensional mapping beneath 15 µm depth. The data provide a direct insight into the internal structure of the examined acritarch microfossils. A three-dimensional dataset was reconstructed from the horizontal slices with VOLVIEW 3 (Kitware Inc. Clifton Park, NY). Bands were assigned according to Raman databases: RASMIN (Raman Spectra Database of Minerals and Inorganic Materials, http://riodb.ibase.aist.go.jp/rasmin/E_index.htm) and RUFF (http://rruff.info/). Hematite and iron oxide bands were assigned according to [36,37].

In addition, the system was equipped with a head for atomic force microscopic imaging, which allowed measurement of the same sample position consecutively with both techniques. The AFM was mounted beneath a 10× objective (Nikon, air) and was operated in tapping mode using back-side gold-coated cantilevers (Nanosenors, PPP-NCT-Au, <10 nm tip radius). The sample was scanned with a 100×100×20 $µm^3$ scan table for both techniques.

Observations and results

Upon lithification, the microfossils were embedded in early diagenetic chert that preserved their three-dimensional structure. The cherty matrix was composed of cryptocrystalline and mostly homogenous quartz with a small admixture of phyllosilicate minerals (clays). The size of the quartz crystallites varied between 1 and 6 µm. Acritarch microfossils with internal bodies were best recognisable in petrographic thin sections with a thickness between 28 and 32 µm. The diameter of the internal bodies was larger in fossils with only two to four internal bodies than in fossils in which more internal bodies occurred. The internal bodies usually occurred in groups and often almost entirely filled the vesicle.[4] In thin sections of early Silurian cherts, most of the acritarchs with spherical internal bodies have been identified as

representatives of sphaeromorph acritarchs, which are classified as belonging to the common form-genus *Leiosphaeridia.* Acanthomorph and herkomorph acritarchs enclosing internal bodies have also been observed (Fig. 2(a,b)). Under the transmitted light microscope, the internal bodies emerged as brownish (Fig. 2(a)) or translucent spheroids with barely visible organic parts (Fig. 2(b)). Although translucent bodies may look like abiotic mineral grains, Raman mapping has revealed that they are enclosed within thin carbonaceous envelopes and has thus confirmed their biological origin.

Scanning electron microscopy (SEM) was used to investigate the surface morphology and elemental composition of microfossils and their fragments. In SEM imaging, the acritarch cell walls were usually distinctly recognisable. The most typical mode of preservation was mineralisation of the organic cell wall by silica, which was often associated with phyllosilicate minerals (Fig. 2). The SEM images showed that the crystallites around and within the acritarchs had a different spatial organisation than those forming the chert matrix (Fig. 2(d)). Very often, crystallites around the cell walls were radially oriented, whereas those forming the matrix occurred in a random orientation. In Archean cherts, this would be an excellent reason to assume that these crystallites are not primary silica-permineralised fossils but are instead the result of diagenetic or metamorphic crystallisation. In the Paleozoic, however, there is no doubt that such crystallites are associated with organic-walled acritarchs. Kempe et al.[28] have also observed that the chert within the acritarch body can be radially oriented.

Elemental composition and distribution were obtained by EDAX analyses. Figure 2(c,d) presents results obtained from chert etched with various hydrofluoric acid concentrations. The same type of cherty rock had variable susceptibility to acid treatment, as shown in Fig. 2, which resulted in more strongly or weakly etched cherts. Embedded microfossils are from Döbra (Frankenwald, Germany, Fig. 2(d)) and, for comparison with Early Silurian specimens from the Sudetes Mountains, Poland (Fig. 2(c)).[4] The different reactions to acid treatment resulted from the varying sizes of SiO_2 crystallites and their contamination with other minerals, especially carbonaceous material.

A variety of microfossils were analysed with confocal Raman spectroscopy to obtain chemical distribution maps of carbonaceous material and minerals (Fig. 3). Figure 4 outlines the Raman spectra used for compositional mapping and shows the spectra for hematite, quartz and kerogenous carbon. An average of about 30 spectra is shown in position A. These data permitted a more detailed correlation of organic parts and surrounding mineral materials with structural elements. To obtain three-dimensional maps, horizontal slices were taken at different focal depths (Fig. 5). In addition, volume images for the three-dimensional distributions of carbonaceous material (D1), quartz and Rayleigh scattering were reconstructed from the slices. This method allowed us to study the acritarchs embedded underneath the chert surface. Horizontal and vertical slices were acquired from the surface to a maximum depth of 5 µm. Raman mapping revealed iron oxide (haematite, 218.2 cm^{-1}, 288.9 cm^{-1}, 402.1 cm^{-1} and 1290 cm^{-1}) and quartz (SiO_2, fundamental mode at 470.1 cm^{-1}) mineralisation in the carbonaceous cell wall remains. In addition, the symmetric stretch peak of CO_3 (1084.4 cm^{-1}) was present, most likely originating from aragonite (~1085 cm^{-1}). The peak at 138.9 cm^{-1} may have its origin from anatase (TiO_2, fundamental mode at ~144 cm^{-1}), a quartz-accompanying mineral, or aragonite (~154 cm^{-1}). All reference peak values were taken from the Raman database RRUFF[33] and [36,37]. The broad carbonaceous material Bands D1 (at about 1340 cm^{-1}), G (at about 1610 cm^{-1}), S1 (at about 2670 cm^{-1}) and S2 (at about 2940 cm^{-1}) were found within the preserved organic parts of the cell. Most of the band assignments are shifted most likely due to high power density from a laser excitation source

that can cause excessive local heating of sample during a Raman experiment (temperature-induced shifts of Raman bands). This is particularly true for iron oxides and oxyhydroxides which can lead to sample transformation which will thus produce a shift, and perhaps also broadening, in Raman bands. An animated three-dimensional reconstruction of a fossil with a similar internal structure is presented as Supporting Information (Fig. S1-S3).

Our measurements demonstrated that the walls of the internal bodies are much thinner than the walls of the acritarch mother vesicles. Raman mapping of carbonaceous material confirmed that carbon is abundantly represented in the cell walls of the acritarch mother vesicle but is less concentrated in the walls of the internal bodies. The cell walls of the internal bodies, like the walls of acritarch mother cells, are mineralised by silica and iron oxides.

Polished thin sections were imaged with AFM. Very similar structures composed partly of silica (quartz) and carbonaceous matter were found on the slightly etched fossil surfaces (5% HF for 3-5 minutes) of the cell walls of both the internal bodies and the acritarch vesicles. Wall thickness emerged as the main difference between the internal body wall and acritarch vesicle wall. The AFM images of these organic-walled microfossils revealed the submicron-scale organisation of kerogenous components of the internal structures. Topographical maps of acritarchs have typically indicated the non-continuous nature of the acritarch walls (Fig. 6). The characteristic platelet (sheeted) structures were well-recognisable (Fig. 6, bottom). Platelets with an average thickness of 30 nm were arranged in a tile-like fashion and locally preserved within the cell wall only. Kempe et al. [27] has suggested that these platelets consist of carbonaceous material and represent the crystalline phase of aromatic hydrocarbons.

Discussion

Even the strongly degraded organic walls of the internal bodies (i.e., spores), which are hardly discernible with optical microscopy, were detectable with Raman microscopy. This type of internal body is extremely rarely preserved in acritarchs as a consequence of the extremely thin (2 to 59 nm)[39,40,41] cell walls of autospores and aplanospores in many modern chlorococcalean algae that are only rarely strengthened by more resistant biomacromolecules like sporopollenin and algaenan[11] making them resistant to decomposition processes.[42,43] Thus, a purely diagenetic (i.e., abiotic) origin of the acritarch internal bodies can be excluded.

Optical micrographs and Raman images showed that the cell walls of only a few of the microfossils enclosing internal bodies were slightly ruptured. The internal structures were individual, separate bodies and could not have originated from the folded (invaginated) fragments of the acritarch mother cell wall. The internal structures were spatially distributed randomly within the acritarch mother vesicle and cannot be considered foreign bodies that entered the acritarchs post mortem. Based on Raman mapping, the following modes of preservation of the cell walls and their internal bodies in early Silurian acritarchs could be distinguished (Fig. 3 and 5): (i) the walls of acritarchs and internal bodies can be preserved as carbonaceous structures permineralised with silica, (ii) the walls of acritarchs and their internal bodies can be preserved as organic material permineralised with silica and iron oxide minerals, or (iii) the organic walls of the internal bodies can be poorly preserved (or not preserved) and can contain less kerogenous matter while the internal bodies are conserved as spheroid structures composed of silica, iron oxide or pyrite.

Additionally, AFM mapping disclosed complementary information concerning the modes of preservation, which are only indistinctly visible by SEM. This information included the

presence or absence of mineral infilling in the internal bodies. As shown on Fig. 6, some of the internal bodies were empty and only their mineralised walls were preserved.

For both the organic (carbonaceous) cell walls and the cell walls of internal bodies, Raman analyses revealed mineralisation by two mineral phases: silica and iron oxides. Based on SEM/EDAX analyses of spherical Precambrian acritarchs, Kempe et al.[28] pointed out that Fe-/Al-, Mg-, K- and Ca-bearing minerals such as carbonates, phyllosilicates and feldspar display a discontinuous and irregular distribution and therefore do not play any role in the fossilisation process of these microfossils. Our observations, based on mineral Raman mapping, conversely suggest that silica, iron oxides and other minerals such as TiO_2 that are bound to acritarch walls play a significant role in preserving the morphology of the acritarchs and their internal bodies (Fig. 3 and 5). In all Raman maps, the distribution of carbonaceous material coincided with the distribution of iron oxides. This observation suggested that mineralisation enabled the preservation of the extremely thin-walled internal structures that otherwise would not have survived the post mortem degradation processes.

In complementary EDAX analyses of the acritarchs studied here, the presence of iron in the walls of internal bodies could not be clearly verified. However, this may be explained by potentially very low iron concentrations, thin cell and especially internal body walls, or by the possible binding of iron to other minerals (quartz, carbonates). In contrast to EDAX and SEM, the confocal Raman microscope penetrates samples to a greater depth and thus integrates over a larger, untreated volume.

The characteristic platy ultrastructure of the kerogenous matter composing the cell walls (Fig. 6) confirmed the results of Kempe at al.[27] and indicated that a common process occurred during the diagenetic transformations of the organics in both cases. The above-described features of the internal bodies and their abundance in the Silurian acritarchs supported the hypothesis that they represent remains of spores and that, as proposed by Kazmierczak and Kremer[4], such spore-bearing acritarchs are consequently not cysts but are instead vegetative cells of microorganisms that are closely affined with modern unicellular green algae (Chlorococcales).

Conclusions

Here we show that the internal bodies in Silurian acritarchs represent organic structures that are intimately associated with the acritarch central body. The three-dimensional mapping enabled observation of the spatial relations between the acritarch body and its internal structures. Because the internal structures often occur in intact acritarchs, and because they are similar to acritarchs in terms of composition, mineralogy and organic wall presence, the internal structures cannot be foreign bodies that entered acritarchs post mortem. Confocal Raman mapping of whole acritarch specimens showed that the internal bodies also cannot be folded parts of the acritarch wall. Like acritarch cell walls, the walls of the internal bodies are often mineralised by silica and/or iron oxide. This conclusion confirmed our earlier suggestion[4] that many acritarchs are unicellular green algae and that the internal bodies represent their asexual reproductive structures (spores). To our knowledge, the c. 420 Ma-old specimens shown in this report represent the earliest thus far described sporulating unicellular green algae (Chlorococcales).

We are aware that our findings have also bearing on the ongoing discussion concerning the biological affinities of phosphatic microfossils from the Neoproterozoic (Ediacaran) Doushantuo Formation of south China described originally as post mortem phosphatized volvocalean-like green algae [44,45] or resting eggs and blastula embryos of early animals

[46,47,48,49,50]. Interestingly, these microfossils have recently been also interpreted as remnants of giant bacteria comparable to modern sulphur bacteria of the genus *Thiomargarita* [51,52]. This idea has been dismissed by showing "embryo-like" Doushantuo fossils inside large acanthomorph acritarchs which, on this basis, have been interpreted as diapause egg cysts [53]. In light of observations of a variety of Paleozoic acanthomorph and other acritarchs enclosing auto- and aplanospore-like internal bodies described by Kazmierczak and Kremer[4], it is possible that the Doushantuo spiny "egg cysts" and "embryos" may represent various developmental stages of similarly asexually reproducing (sporulating) unicellular green algae. We shall discussed details of this interesting topic in a separate paper.

This study also demonstrated that confocal Raman spectroscopy is a powerful tool for the investigation of organic structures entombed within a mineral matrix. Three-dimensional compositional Raman data are complementary to data obtained by SEM and optical microscopy. Confocal Raman spectroscopy is non-destructive and provides a high level of resolution, which is often critical for rare and uniquely preserved paleontological material. The combination of micro- and nanoanalytic techniques helps to elucidate even the finest structures of microfossils and to discriminate between true fossils and pseudofossils.[54] This information is particularly important in the case of purported traces of life in the oldest rocks.

Acknowledgments

We are grateful to Madeleine Fischer (LMU Munich) and Zbigniew Strak (PAS, Warsaw) for making thin sections. The Department of Earth and Environmental Sciences and the GeoBio-Center of LMU Munich are generously acknowledged for offering working facilities. BK was supported by the Alexander von Humboldt Foundation.

References:

[1] C. Downie, W. R. Evitt, W. A. S. Sarjeant, *Stanford Univ Publ Geol Sc.* 1963, **7**, 3.

[2] F. Martin, *Bio Rev.* 1993, **68**, 475.

[3] E. J. Javaux, A. H. Knoll, M. R. Walter, *Geobiology.* 2004, **2**,121.

[4] J. Kazmierczak, B. Kremer, *Acta Palaeont Pol.* 2009, **54**,541.

[5] P.K. Strother in: *Palynology: Principles and Applications*, (Eds: J. Jansonius, D.C. McGregor), American Association of Stratigraphic Palynologists Foundation, Salt Lake City 1996, pp.81-106.

[6] N. M. Talyzina, M. Moczydlowska, *Rev Palaeo Palyn.* 2000, **112**,1.

[7] S. Willman, M. Moczydlowska, *Lethaia.* 2007, **40**,111.

[8] S. Willman, *Geobiology.* 2009, **7**,8.

[9] K. Arouri, P. F. Greenwood, M. R. Walter, *Org Geochem.* 1999, **30**,1323.

[10] K. Arouri, P. F. Greenwood, M. R. Walter, *Org Geochem.* 2000, **31**,75.

[11] A. W. Jr Atkinson, B. E. S. Gunning, P. C. L. John *Planta.* 1972, **107**,1.

[12] J. Burczyk, B. Śmietana, K. Termińska−Pabis, M. Zych, P. Kowalowski, *Phytochemistry.* 1999, **51**,491.

[13] A. Eisenack, *N Jb Geol Paläont Abh.* 1968, **131**,1.

[14] S. Lindgren, *Stockholm Contr Geol.* 1981, **38**,1.

[15] C. P. Marshal, E. J. Javaux, A. H. Knoll, M. R. Walter, *Precambr Res.* 2005, **138**,208.

[16] J. W. Schopf, A. B. Tripathi, A. B. Kudryavtsev, *Astrobiology.* 2006, **1**,1.

[17] J. W. Schopf, A. B. Kudryavtsev, *Precambr Res.* 2009, **173**,39.

[18] A. B. Kudryavtsev, J. W. Schopf, D. G. Agresti, T. J. Wdowiak, *Proc Natl Acad Sci USA*, 2001, **98**, 823.

[19] J. W. Schopf, A. B. Kudryavtsev, D. G. Agresti, A. D. Czaja, T. J. Wdowiak, *Astrobiology.* 2005, **5**,333.

[20] J. W. Schopf, A. B. Kudryavtsev, A. D. Czaja, A. B. Tripathi, *Precambr Res.* 2007, **158**, 141.

[21] J-Y. Chen, J. W. Schopf, D. J. Bottjer, C-Y. Zhang, A. B. Kudryavtsev, A. B. Tripathi, X-Q. Wang, Y-H. Yang, X. Gao, Y. Yang, *Proc Natl Acad Sci USA.* 2007,**104**,6289.

[22] M. D. Brasier, O. R. Green, A. P. Jepcoat, A. K. Kleppe, M. J. Van Kranendonk, J. F. Lindsay, A. Steele, N. V. Grassineau, 2002. *Nature* **247**, 76.

[23] J. D. Pasteris, B. Wopenka, 2002. *Nature* **420**, 476.

[24] J. D. Pasteris, B. Wopenka, 2003. *Astrobiology* **3**, 727.

[25] C. P. Marshall, H. G. M. Edwards, J. Jehlicka, 2010. *Astrobiology* **10**, 229.

[26] H. Chi, Z. Xiao, J. Chen, Z. Lu, *Scanning* 2007, **29**,102.

[27] A. Kempe, J. W. Schopf, W. Altermann, A. B. Kudryavtsev, W. Heckl, *Proc Natl Acad Sci USA* 2002; **99**, 9117.

[28] A. Kempe, R. Wirth, W. Altermann, R. W. Stark, J. W. Schopf, W. M. Heckl, *Precambr Res.* 2005, **140**, 36.

[29] J. Komárek , B. Fott, *Das Phytoplankton des Süßwassers*, E. Schweizerbart'sche Verlagsbuchhandlung, Stuttgart, 1983.

[30] D. J. Hibberd, in *Handbook of Protoctista*, (Eds: L. Margulis, J. O. Corliss, M. Melkonian, and D. J. Chapman), Jones and Barlett Publishers, Boston, 1990, pp. 686-697.

[31] G. K. Colbath, H. R. Grenfell, 1995. *Rev Palaeobot Palynol*., **86**, 287.

[32] W. Franke, *J Geol Soc London Spe Publ.* 1984, **14**, 33.

[33] V. Stein, *N Jb Geol Paläont, Abh.* 1965, **121**,111.

[34] G. Horstig, G. von Stettner, *Bayer Geol Landesamt, München.* 1976, 1.

[35] V. Herrmann, *Untersuchungen zur Sedimentation, Diagenese und Deformation der silurischen Sedimentgesteine im Gebiet westlich der Münchberger Gneismasse* [unpubl]. Diploma thesis, Techn Univ Darmstadt, 1999.

[36] I. Chamritski, G. Burns, *J Phys Chem* B 2005,**109**, 4965.

[37] D.L.A.d. Faria, S.V. Silva, M.T.d. Oliveira, *J Raman Spectrosc* 1997, **28**, 873.

[38] R. T. Downs, *Program and Abstracts of the 19th General Meeting of the International Mineralogical Association in Kobe, Japan*. 2006, O03.

[39] E. Hegewald, E. Schnepf, *Nova Hedwigia* 1984, **39**, 297.

[40] M. Yamamoto, M. Fujishita, A. Hirata, S. Kawano, *J Plant Res* 2004,**117**, 257.

[41] M. Yamamoto, I. Kurihara, S. Kawano, *Planta* 2005, **221**, 766.

[42] S. Derenne, C. Largeau, C. Berkaloff, B. Rousseau, C. Wilhelm, P. G. Hatcher, *Phytochemistry* 1992, **31**, 1923.

[43] J. W. de Leeuw, G. J. Versteegh, P. F. van Bergen, *Plant Ecology* 2006, **182**, 209.

[44] Y. Xue, T. Tang, C. Yu, C. Zhou, C. *Acta Palaeont Sinica* 1995, **34**, 688.

[45] Y. Xue, C. Zhou, T. Tang, 1999, *Acta Micropaleont Sinica* 1999, **16**, 1.

[46] S. Xiao, A.H. Knoll, *J Paleont*. 2000, **74**, 767.

[47] S. Xiao, Y. Zhang, A. H. Knoll, *Nature* 1998, **315**, 655.

[48] S.Xiao, X. Yuan, A. H. Knoll, A.H., *Proc Natl Acad Sci USA* 2000, **97**, 13684.

[49] C. Yin, S. Bengtson, Z. Yue, *Acta Palaeont Polonica* 2004 **49**,1.

[50] C. Yin, M. Zhu, A.H. Knoll,X. Yuan, J. Zhang, J. Hu, J., *Nature* 2007, **446**, 661.

[51] S. Q. Dornbos, D. J. Bottjer, J. Y. Chen, P. Oliveri, F. Gao, C.W. Li, *Lethaia* 2005, **38**, 101.

[52] J. V. Bailey, S. B. Joye, K. M. Kalanetra, B. E. Flood, F. A. Corsetti, *Nature* 2007, **445**, 198.

[53] J. V.Bailey, S.B. Joye, K.M. Kalanetra, B.E. Flood, F. A. Corsetti, F.A., *Nature* 2007, **446**, E9.

[54] J. W. Schopf, A. B. Kudryavtsev, K. Sugitani, M. R. Walter, *Precambr. Res.* 2010, **179**,191.

Figure legends

Fig. 1. Geographical location of the study area. The star indicates the sampling outcrop.

Fig. 2. Acritarchs from early Silurian cherts. A and B: transmitted light micrographs of acritarchs with internal bodies (spores) preserved as a combination of organic matter and minerals, Döbra (Frankenwald, Germany). The internal bodies in (A) have well-preserved organic walls, whereas in (B), the organic walls are highly degraded but still visible. C and D: SEM images representing typical modes of preservation in polished and HF-etched samples. C: Example of 3D-etched acritarchs from the cherty matrix, Lupianka (Sudetes Mountains, Poland). D: HF–etched cross-section of an acritarch with internal bodies; visible is a rim of radially oriented quartz crystallites close to the vesicle wall and of fine crystalline silica in the middle. EDAX spectrum collected from the acritarch wall (arrowed inset), Döbra (Frankenwald, Germany).

Fig. 3. Confocal Raman microscopy of an acanthomorph acritarch. The image size is 70×70 µm^2 with 220×220 spectra. All spectra were obtained with an integration time of

0.07 s. (a) Compositional map generated with a sum filter (1225-1450 cm^{-1}) representing the carbon D1 band, (b) calculated for the hematite peak (210–235 cm^{-1}), and (c) for quartz (SiO_2, 445-493 cm^{-1}). (d) Overlay of the kerogen (green) with the iron oxide distribution (red), showing that both minerals are localised at the cell wall.

Fig. 4. Typical Raman spectra obtained on the cell remains as indicated in the inset. Important peaks are labelled. Spectrum A represents an average over 30 spectra around the location indicated by the arrow. Spectra B and C are diffraction-limited, single-point spectra. The relative peak intensities (literature values) of characteristic minerals are indicated with black (high intensity), grey (medium) and white (weak) boxes below. Inset: Optical micrograph of the acritarch in thin section. The arrows indicate the location of the spectra.

Fig. 5. Distribution of carbonaceous material in early Silurian sphaeromorph acritarchs (Döbra, Frankenwald) with internal bodies in depth profiling. (a1) and (b1) are optical micrographs; the other images represent horizontal Raman slices at different depths, each with a height divergence of 0.5 µm. The kerogen (D1 band) distribution was used to generate the images. (a2-a8): image size 70×70 $µm^2$; 300×300 spectra; integration time 0.06 s. (b2-b8): image size 60×60 $µm^2$; 220×220 spectra; integration time 0.08 s. With increasing depth, supplementary internal structures become consecutively visible. The white bar indicates 10 µm. The images on the right outline three-dimensional data of the kerogen D1 band, quartz and elastic scattering (Rayleigh) that were reconstructed from the slices.

Fig. 6. Top: AFM images of a sphaeromorph acritarch with internal bodies. The higher resolution images reveal internal bodies with thin organic envelopes that are composed of patchy, very fine-grained kerogen. a and b: transmitted light photograph, c: surface topography image, d: phase image of an internal body (spore) with topography (e).
Bottom: AFM images of an acanthomorph acritarch with internal bodies showing a distinct organic cell wall visible as imbricate platelets (magnified in a and b), c: surface topography image, d: magnified internal body (spore), e: phase image of a compacted internal body (spore).

Figure 1. Geographical location of the study area. The star indicates the sampling outcrop

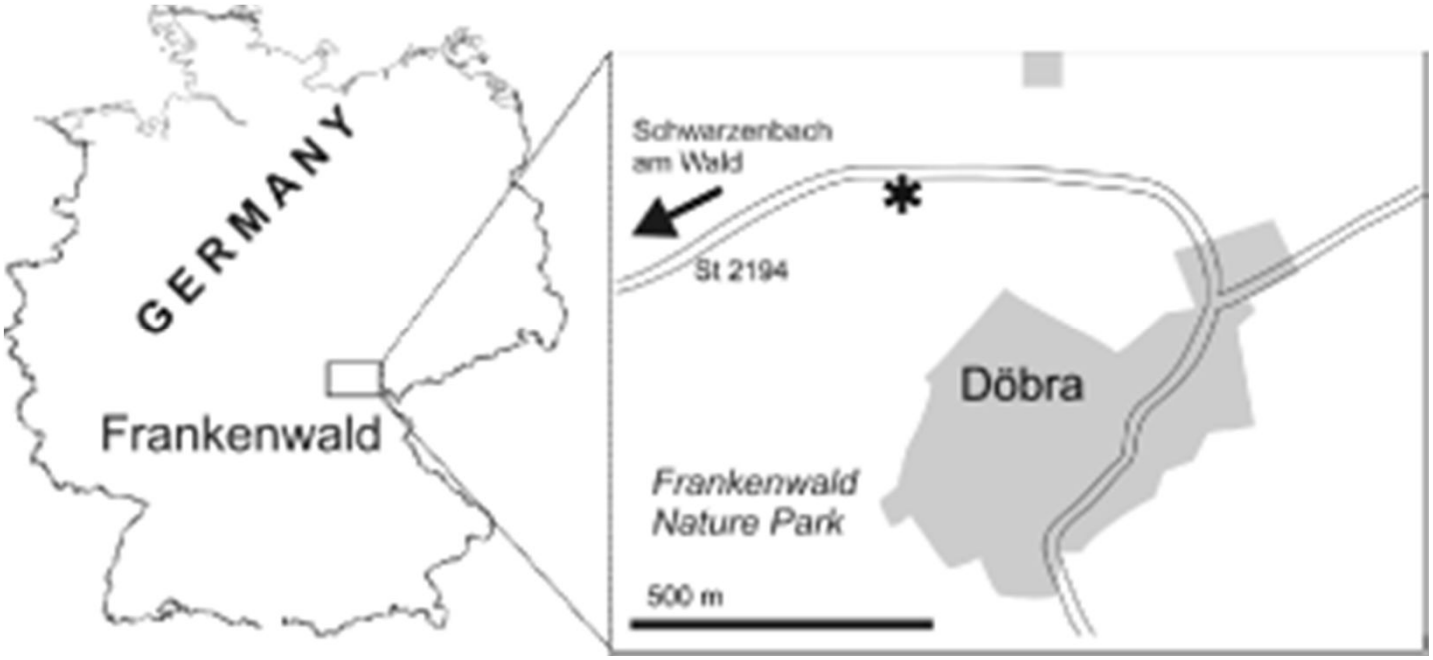

Figure 2. Acritarchs from early Silurian cherts. (a and b) Transmitted light micrographs of acritarchs with internal bodies (spores) preserved as a combination of organic matter and minerals, Döbra (Frankenwald, Germany). The internal bodies in (a) have well-preserved organic walls, whereas in (b), the organic walls are highly degraded but still visible. (c and d) SEM images representing typical modes of preservation in polished and HF-etched samples. (c) Example of 3D etched acritarchs from the cherty matrix, Lupianka (Sudetes Mountains, Poland). (d) HF-etched cross-section of an acritarch with internal bodies; visible are a rim of radially oriented quartz crystallites close to the vesicle wall and of fine crystalline silica in the middle. EDAX spectrum collected from the acritarch wall (arrowed inset), Döbra (Frankenwald, Germany)

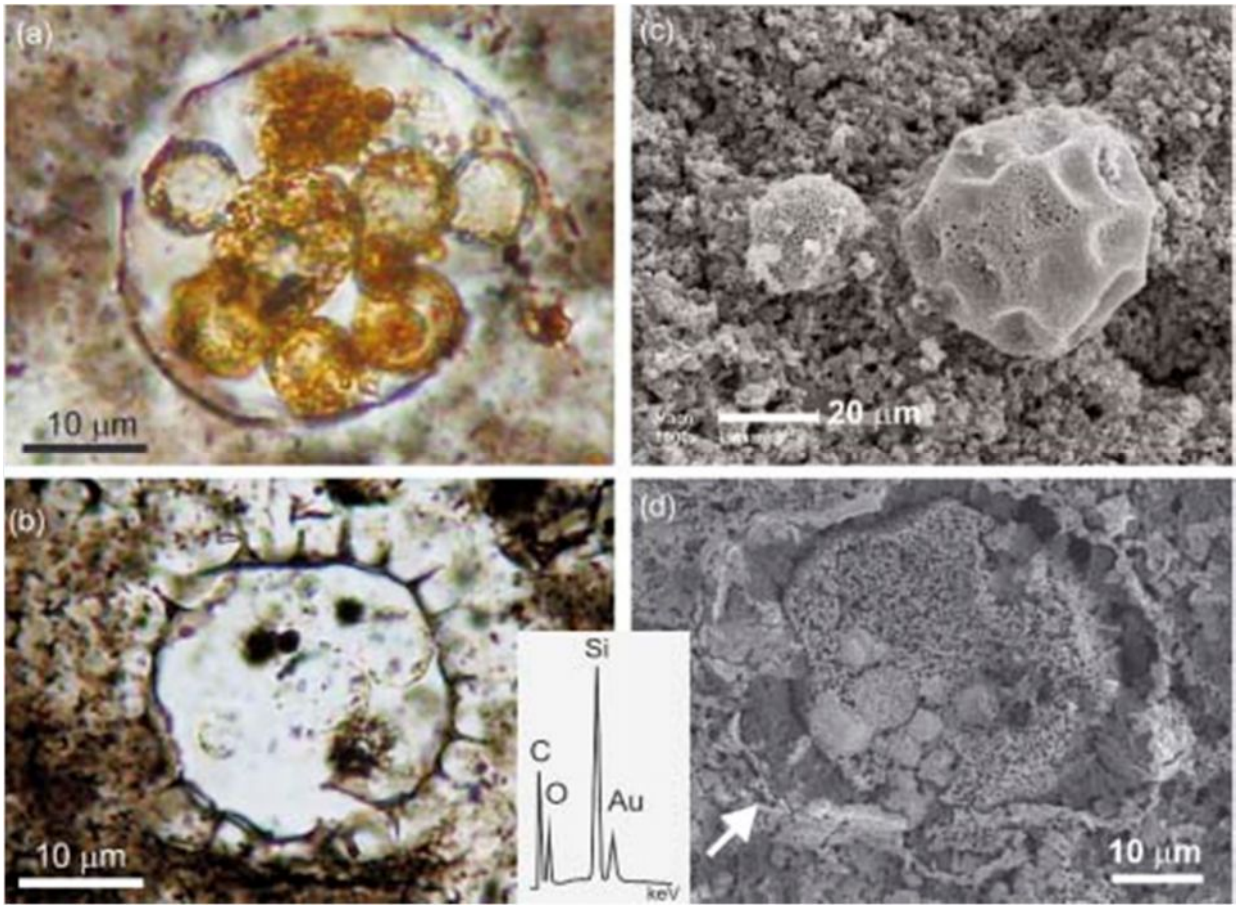

Figure 3. Confocal Raman microscopy of an acanthomorph acritarch. The image size is 70 × 70 μm^2 with 220 × 220 spectra. All spectra were obtained with an integration time of 0.07 s. (a) Compositional map generated with a sum filter (1225–1450 cm^{-1}) representing the carbon D1 band, (b) calculated for the hematite peak (210–235 cm^{-1}), (c) for quartz (SiO_2, 445–493 cm^{-1}), and (d) overlay of the kerogen (green) with the iron oxide distribution (red), showing that both minerals are localised at the cell wall

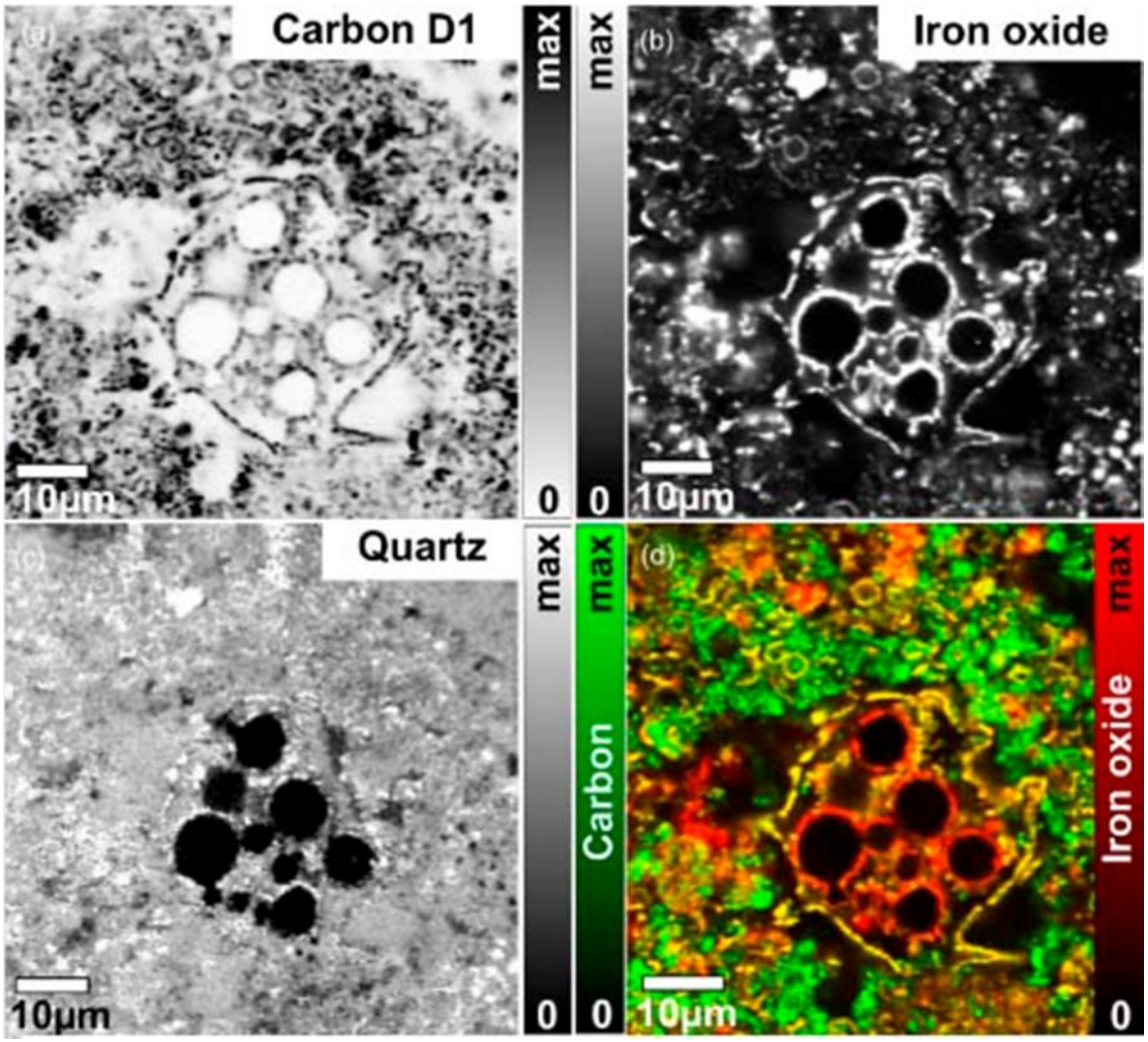

Figure 4. Typical Raman spectra obtained on the cell remains as indicated in the inset. Important peaks are labelled. Spectrum A represents an average over 30 spectra around the location indicated by the arrow. Spectra B and C are diffraction-limited, single-point spectra. The relative peak intensities (literature values) of characteristic minerals are indicated with black (high intensity), grey (medium) and white (weak) boxes below. Inset: Optical micrograph of the acritarch in thin section. The arrows indicate the location of the spectra

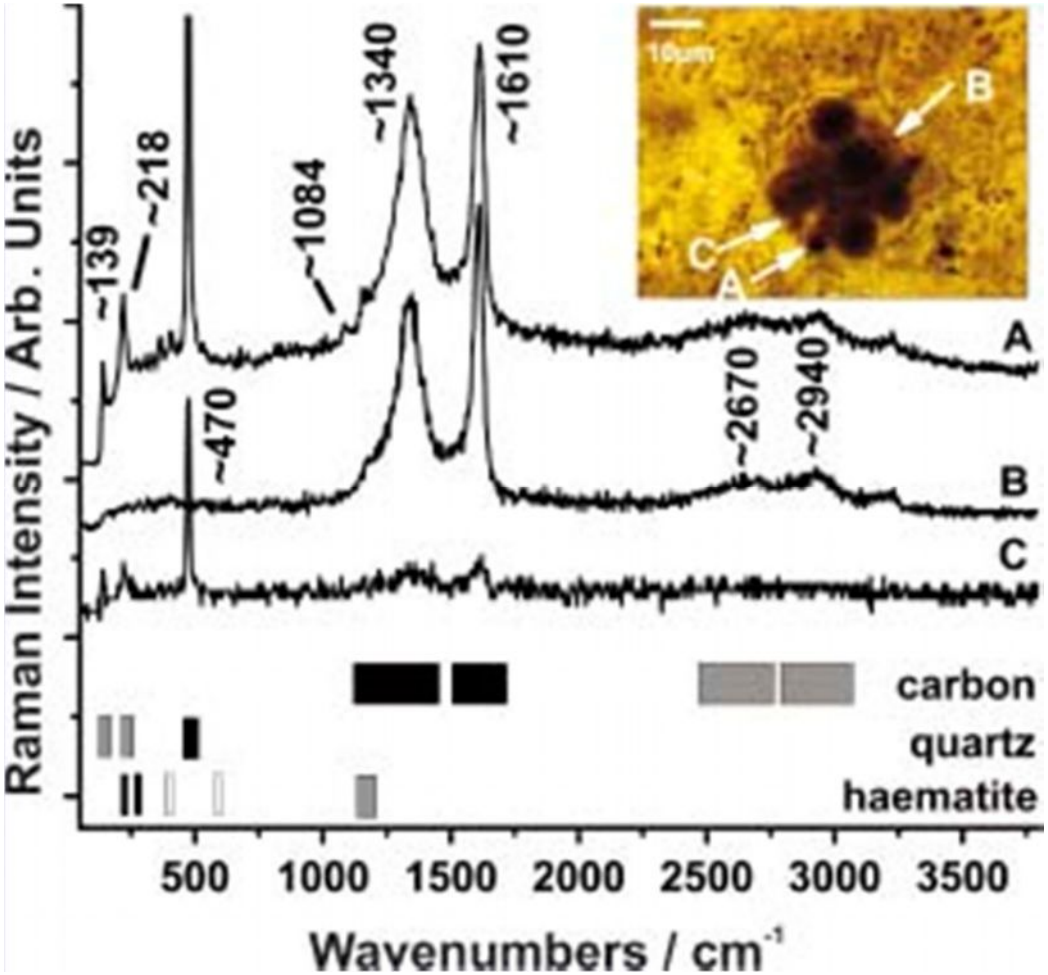

Figure 5. Distribution of carbonaceous material in early Silurian sphaeromorph acritarchs (Döbra, Frankenwald) with internal bodies in depth profiling. (a1) and (b1) are optical micrographs; the other images represent horizontal Raman slices at different depths, each with a height divergence of 0.5 µm. The kerogen (D1 band) distribution was used to generate the images. (a2–a8): image size 70 × 70 µm^2; 300 × 300 spectra; integration time 0.06 s. (b2–b8): image size 60 × 60 µm^2; 220 × 220 spectra; integration time 0.08 s. With increasing depth, supplementary internal structures become consecutively visible. The white bar indicates 10 µm. The images on the right outline three-dimensional data of the kerogen D1 band, quartz and elastic scattering (Rayleigh) that were reconstructed from the slices Supporting Information (Figs S1-S3)

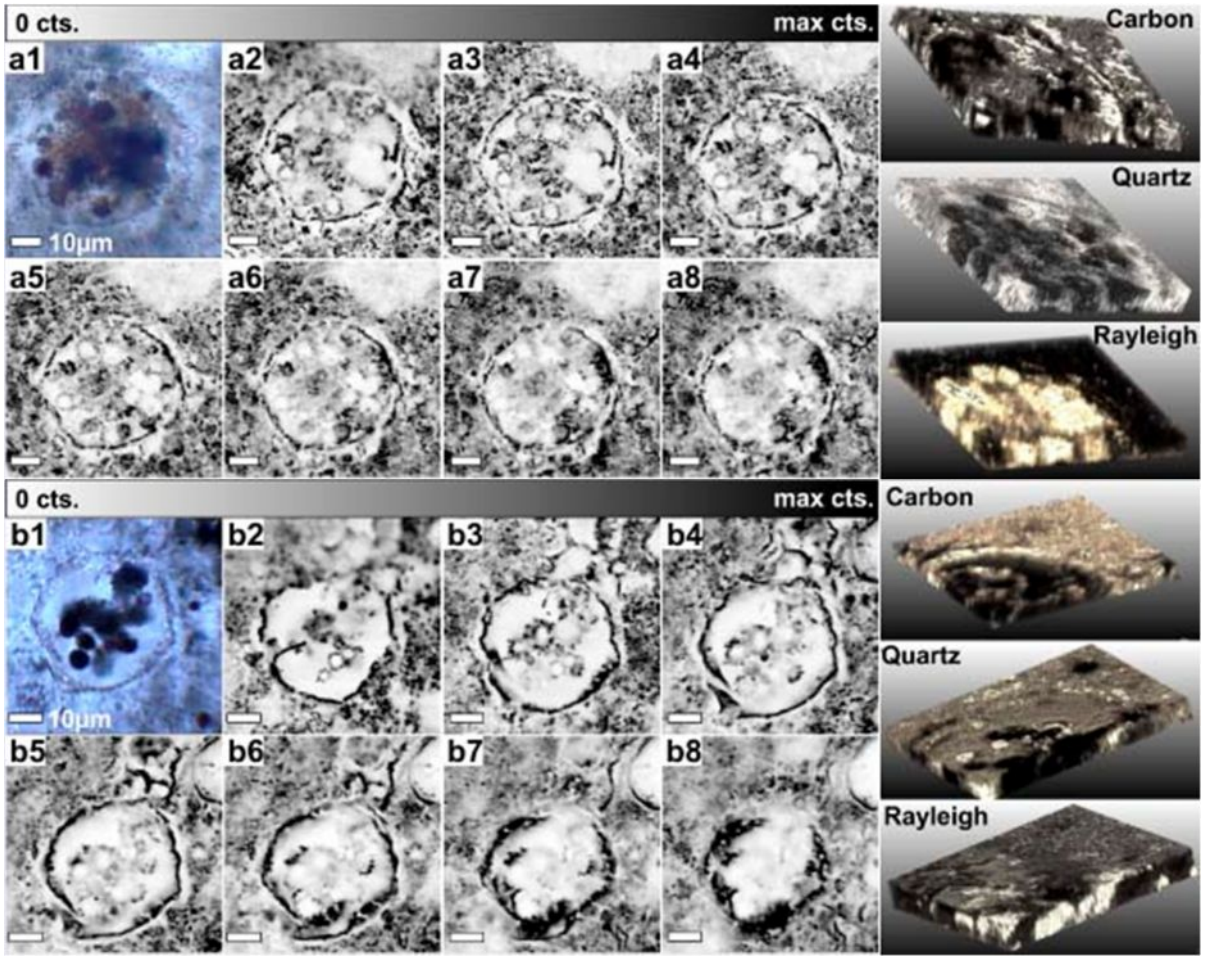

Figure 6. Top: AFM images of a sphaeromorph acritarch with internal bodies. The higher resolution images reveal internal bodies with thin organic envelopes that are composed of patchy, very fine-grained kerogen. (a) and (b): transmitted light photograph, (c): surface topography image, (d): phase image of an internal body (spore) with topography (e). Bottom: AFM images of an acanthomorph acritarch with internal bodies showing a distinct organic cell wall visible as imbricate platelets (magnified in (a) and (b)), (c): surface topography image, (d): magnified internal body (spore), (e): phase image of a compacted internal body (spore)